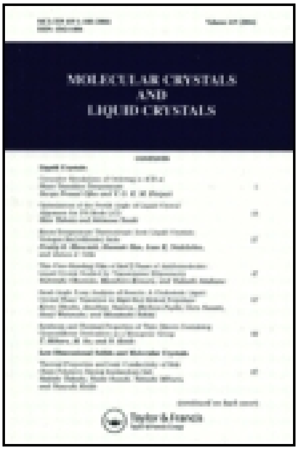

Molecular Crystals and Liquid Crystals Science and Technology. Section A. Molecular Crystals and Liquid Crystals

Publication details, including instructions for authors and subscription information:
http://www.tandfonline.com/loi/gmcl19

Photogeneration in an Acceptor-Type Poly(Phenylenevinylene)

D. Hertel [a] , H. Bässler [a] , S. Möller [b] , H. Tillmann [c] & H. H. Hörhold [c]

[a] Institute of Physical, Nuclear and Macromolecular Chemistry and Material Science Centre, Philipps-University Marburg, Hans-Meerwein-Strasse, 35032, Marburg, Germany

[b] Department of Physics, Philipps-University Marburg, Renthof 5, 35037, Marburg, Germany

[c] Institute of Organic and Macromolecular Chemistry, Friedrich Schiller University, 07743, Jena, Germany

To cite this article: D. Hertel, H. Bässler, S. Möller, H. Tillmann & H. H. Hörhold (2001): Photogeneration in an Acceptor-Type Poly(Phenylenevinylene), Molecular Crystals and Liquid Crystals Science and Technology. Section A. Molecular Crystals and Liquid Crystals, 355:1, 175-190

To link to this article: http://dx.doi.org/10.1080/10587250108023660

Mol. Cryst. Liq. Cryst., Vol. 355, pp. 175-190
Reprints available directly from the publisher
Photocopying permitted by license only

Published by license under the
Gordon and Breach Science Publishers imprint.
Printed in Malaysia

Photogeneration in an Acceptor-Type Poly(Phenylenevinylene)*

D. HERTEL[a], H. BÄSSLER[a†], S. MÖLLER[b], H. TILLMANN[c] and H.H. HÖRHOLD[c]

[a]Institute of Physical, Nuclear and Macromolecular Chemistry and Material Science Centre, Philipps-University Marburg, Hans-Meerwein-Strasse, 35032 Marburg, Germany, [b]Department of Physics, Philipps-University Marburg, Renthof 5, 35037 Marburg, Germany and [c]Institute of Organic and Macromolecular Chemistry, Friedrich Schiller University, 07743 Jena, Germany

(Received December 09, 1999; In final form February 11, 2000)

Stationary photoconduction in thin films of a cyano-phenylamine-substituted poly-phenylenevinylene, in both sandwich and gap arrangement, has been studied. In order to separate electrode from bulk effects a thin layer of SiO_x could be inserted between the indium-tinoxide (ITO) electrode and the film. Photocurrents were measured as a function of electric field, temperature (100 to 300K), photon energy (2.5 to 5 eV) and polarity of the applied bias. The results indicate that for $h\upsilon < 3.2$ eV the photocurrent is a superposition of bulk ionization involving relaxed singlet excitons and, depending on the direction of the electric field, exciton induced injection of predominantly electrons from the ITO. For $h\upsilon > 3.2$ eV intrinsic photogeneration from hot singlet excitons takes over.

Keywords: Photoconductivity; Poly(phenylene-vinylene) derivatives

1 INTRODUCTION

Measuring photoconductivity is one of the key experiments to probe optically driven charge carrier production in a semiconductor or insulator. It provides information on the energetics of this process. If photoionization occurs with an efficiency much less than unity and is assisted by electric field and temperature it has to be an endothermic process. Reversing the argument, recombination of a pair of opposite charges, for instance injected from the electrodes, has to be exothermic if efficient. In organic solids this condition is always met because the

---

* Dedicated to the memory of Prof. Edgar Silinsh

† Corresponding Author.

dielectric constant is low and, concomitantly, the Coulombic binding energy of a electron-hole pair is large [1]. It is mainly for this reason why organic light emitting diodes work as efficiently as they actually do.

However, to simply measure a photocurrent in an organic solid is insufficient to delineate the mechanism by which charge carriers are generated. Quite often it is to difficult to distinguish which process is intrinsic in nature rather than related to deliberate or accidental dopants and what is the role of surface effects as compared with bulk effects. As far as conjugated polymers are concerned it is meanwhile well established that the primary excitations are neutral excitons of the Frenkel or Wannier-type. Furthermore the photogeneration efficiency is dependent on electric field and temperature and is much less than unity [2–11]. Phenomenologically the situation appears to be similar to that in molecular crystals in which unipolar charge injection via exciton dissociation at an electrode controls photoconduction near the absorption edge [12] while intrinsic effects prevail at higher excitation energies [13]. Conceptually there must be differences, though, because in an array of extended conjugated polymer segments of a length comparable to the coulombic capture radius, the diffusive escape of an optically generated geminate electron-hole pair must require modification.

In this work we examine the steady state photogeneration in poly[phenylimino-1,4-phenylene-1,2-(2-cyano)-ethenylene-2,5-dioctyloxy-1,4-phenylene-1,2-(1-cyano)-ethenylene-1,4-phenylene] (CN-PA-PPV). Due to the electronegative cyano-functionalities it should behave as an electron acceptor, for instance if combined with an electron donor to form a photovoltaic device [14]. By using a bare ITO as compared to ITO covered with SiO_x as electrode, we are able to differentiate surface from bulk effects and to identify the sign of the majority carriers in the course of injection [5, 6]. Further we confirm that intrinsic intra-chain photogeneration requires excess photon energy as compared with that of the singlet exciton.

2 EXPERIMENTAL

Poly[phenylimino-1,4-phenylene-1,2-(2-cyano)-ethenylene-2,5-dioctyloxy-1,4-phenylene-1,2-(1-cyano)-ethenylene-1,4-phenylene] (CN-PA-PPV) was prepared by polycondensation via Knoevenagel reaction [15]. The synthetic route is depicted in scheme 1 and a detailed description of the synthesis is given below.

4,4'Diformyl-triphenylamine (0.904 g; 3 mmol) and 2,5-dioctyloxy p-xylylene dinitrile (1.237 g; 3 mmol) were dissolved in a mixture of toluene (20 ml) and *tert*-butanol (2 ml) whilst being stirred under argon and heating to reflux. To this solution was added in one portion potassium-*tert*-butoxide (50 mg; 0.45 mmol),

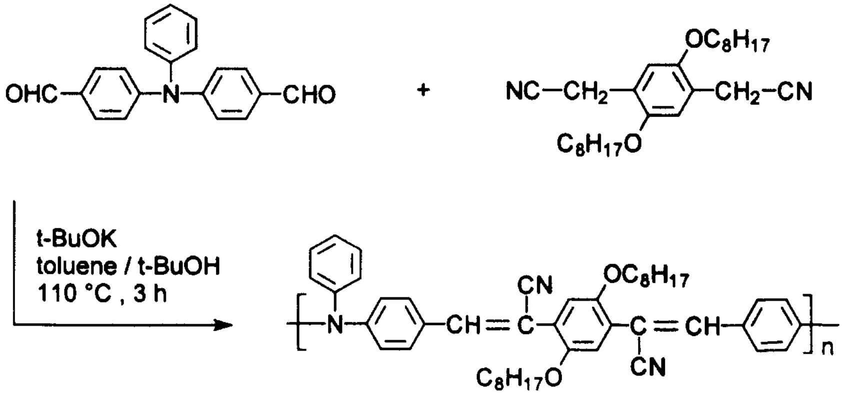

SCHEME 1 Synthesis of CN-PA-PPV via Knoevenagel Condensation Reaction

dissolved in *tert*-butanol (0.5 ml). After 3 h at reflux and subsequent neutralization with acetic acid, the mixture was diluted with additional toluene, filtered, washed several times with distilled water and dried in a Dean-Stark apparatus. The resulting toluene solution was filtered, reduced to a minimum and precipitated into methanol. Then the crude polymer was extracted with methanol for 5 h to separate byproducts and oligomers. Reprecipitation from toluene / methanol gave the orange polymer with a yield of 1.5 g (74 %) after vacuum drying. The glass transition temperature was found to be 78°C (DSC). For analytical data of the polymer see [16].

The devices were handled on ambient conditions and showed no signs of photooxidation during preparation or handling. For photoconduction experiments films of CN-PA-PPV were spin-coated from Chloroform solution (1 % by weight) on top of a conductive 20 nm thick indium tinoxide glass (ITO; Balzers). Before completing the sandwich structure by evaporating a semitransparent aluminium (Al) top contact of 0.07 cm^2 the sample was kept in a vacuum chamber at a pressure of 10^{-6} mbar at 295 K for 12 hours to remove residual solvent. In order to suppress charge carrier injection from the ITO electrode, devices were fabricated carrying a 8 ± 2 nm thin evaporated layer of silicon monoxide (SiO_x; Balzers) on top of the ITO. All other steps of fabrication were identical. The total distance between the electrodes in both sets of devices was 100 nm. To test the influence of electrode related effects further we used devices in a surface geometry with interdigitated platinum electrodes. The gap between the electrodes was 160 μm. From previous work it is known that photocurrents in such a surface geometry are less liable to charge injection from electrodes, although caution has to be taken to avoid bimolecular recombination of charges [2]. Another disadvantage of the surface cell is the difficulty to calculate the quantum efficiency of charge generation, since the 'sweep-out' condition [2] is usually not fulfilled in these devices.

Stationary photocurrent measurements were performed in a temperature controlled cryostat under reduced pressure (10^{-5} mbar) using a calibrated xenon lamp as a light source. A low noise current preamplifier and/or a lock-in amplifier were employed for signal detection. The excitation light was modulated at 384 Hz and no dependence of the photocurrent on the modulation frequency was observed down to 10 Hz. The devices were illuminated through the semitransparent aluminium electrode. Experiments where the device was illuminated through the ITO electrode showed no differences compared with illumination through the Al electrode. All data reported were taken in a pointwise fashion and refer to photocurrents established immediately after light excitation. Although we could not detect any dependence of the photocurrents on the mode of data recording in order to make sure that sample charging was negligible, the sample was shorted and irradiated with red light for two minutes after each measurement before the next data point was taken. Dark currents were typically on the order of 10^{-10} A/cm^2 translating into a dark conductivity $<10^{-15}$ $(\Omega\text{cm})^{-1}$. This is 2 to 3 orders of magnitude less than the dark conductivity of SiO_x [17] indicating that the interfacial resistance is negligible.

Absorption spectra of the films on quartz slides were recorded with a Perkin Elmer UV/VIS/NIR spectrometer at room temperature.

3 RESULTS

In this section we will first illustrate the different results observed upon investigating the influence of SiO_x on the photocurrents in our devices. Second we describe the dependence of the photocurrents on light intensity, temperature and electric field.

The photocurrent action spectra of two different CN-PA-PPV devices recorded at an applied field of 3×10^5 V/cm are presented in fig. 1 together with the absorption spectra of the corresponding films. The inhomogeneous broadened $S_1 \leftarrow S_0$ absorption band exhibits its maximum at 2.75 eV with a slight asymmetry at the high energy tail. At energies of around 4 eV and 4.5 eV transitions to higher excited states appear. The photocurrent action spectra are corrected for the transmittance of the Al electrode and the spectral characteristics of the xenon lamp. The curves in fig. 1(a) display the photocurrents measured with a bare ITO electrode. As it can be seen from fig. 1(a)the photocurrent starts at the absorption

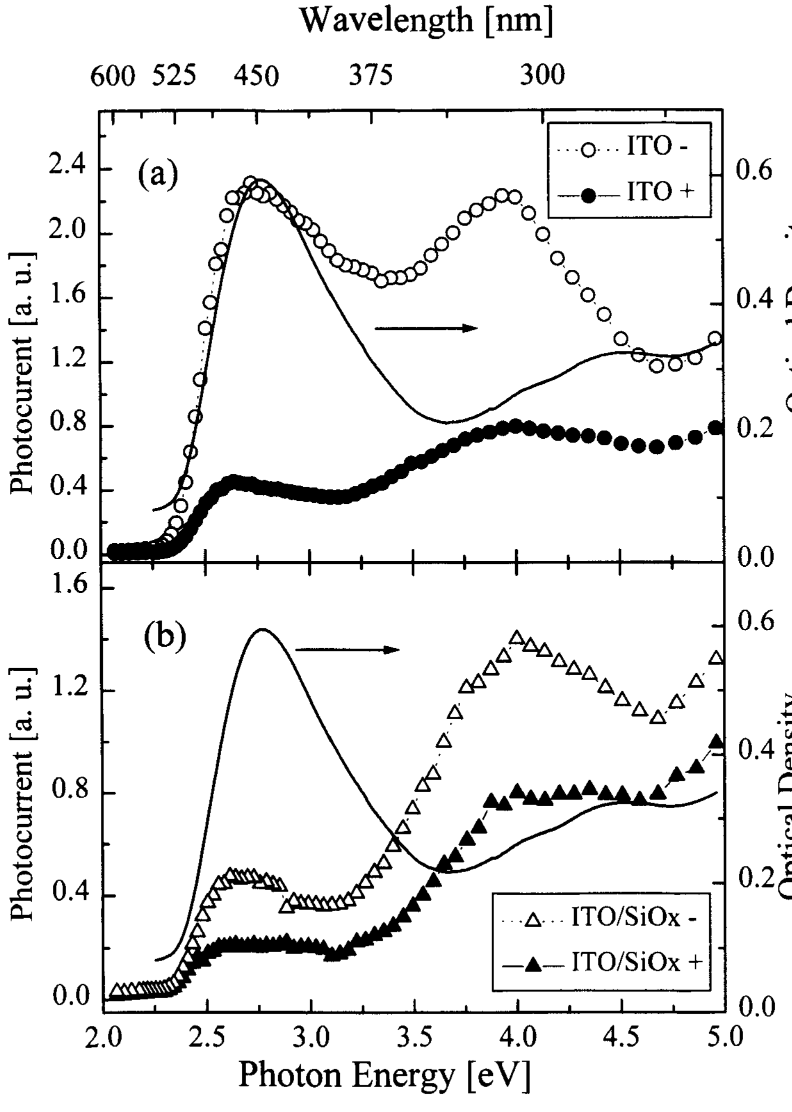

FIGURE 1 Photocurrent action spectra of CN-PA-PPV with bare ITO (a) and ITO/SiO$_x$ (b) at an applied field of 3×10^5 V/cm and room temperature. The solid and open symbols refer to forward and reverse bias respectively. Excitation was done through the semitransparent Al electrode. The solid line is the optical density of the CN-PA-PPV films

edge and reaches a first maximum at the peak of absorption at around 2.7 eV. This so-called symbatic behaviour turns into antibatic behaviour at around 3.2

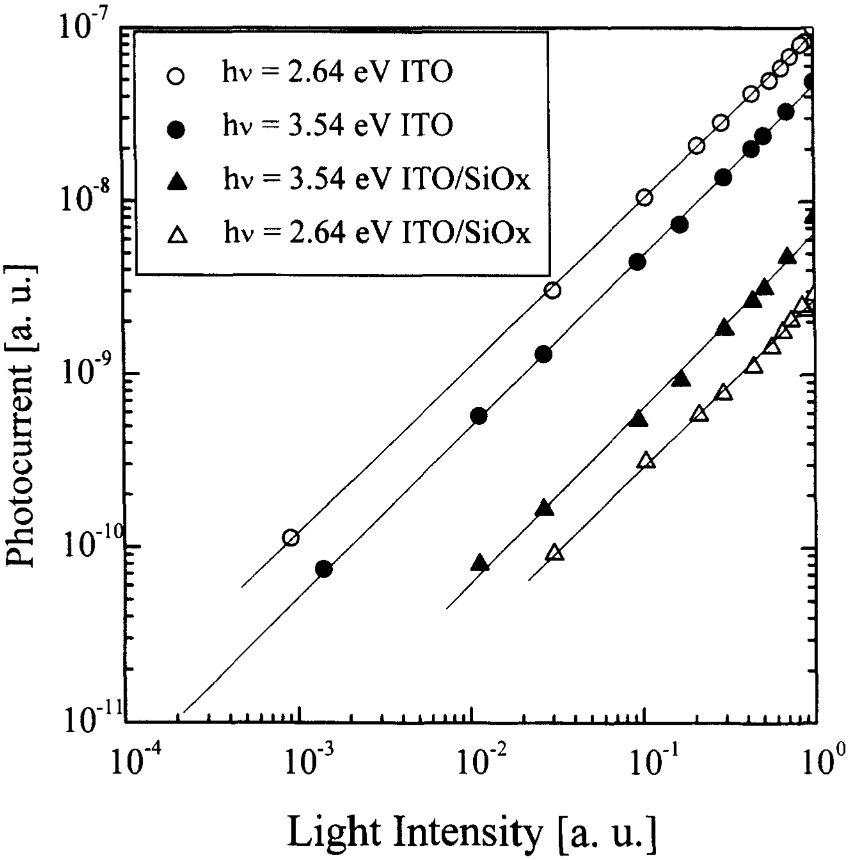

FIGURE 2 Photocurrent vs. light intensity at an applied electric field of 3×10^5 V/cm for different excitation energies (2.64 eV open symbols, 3.54 eV solid symbols). The circles refer to a device with bare ITO, whereas the triangles represent data from the ITO/SiO_xdevice. Excitation was done through the semitransparent Al electrode

eV, i.e. 0.7 eV above the $S_1 \leftarrow S_0$ 0–0 transition located at the tail of the disorder broadened vibronic replica. From 3.2 eV to 4 eV the photocurrent increases further but does not correlate with the absorption in the high energy region of the spectrum. Above 4 eV the current decreases. Another feature as evident from fig. 1(a) is the bias dependence of the photocurrent. It is obvious that the charge generation below 3.2 eV is by a factor of 6 more efficient if the ITO is biased negatively. This difference becomes smaller above 3.2 eV.

Photocurrents measured with a thin SiO_x blocking layer on top of the ITO are shown in fig. 1(b). Compared with the bare ITO device the absolute values of the

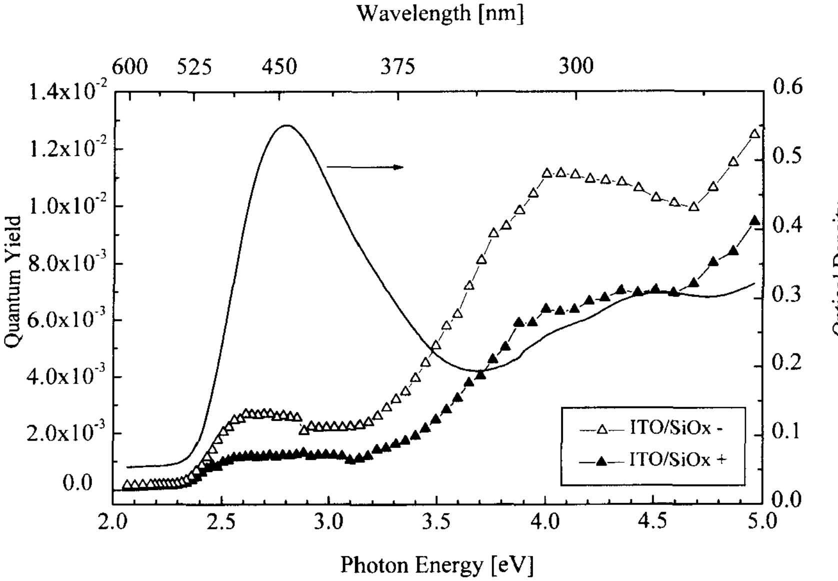

FIGURE 3 The data of fig. 1(b) normalised to the number of absorbed photons

photocurrent under forward bias, i. e. ITO/SiO$_x$ being positive, decrease by a factor of 2 at most, whereas under reversed bias the current is by a factor of 5 to 6 less. However, this difference vanishes above a photon energy of 3.2 eV.

That the measured photocurrent corresponds to the total number of charges generated during excitation is testified by the graph plotted in fig. 2. The applied electric field was 3x10^5 V/cm. For both devices the photocurrent varies linearly with light intensity over three orders of magnitude, implying the absence of bimolecular charge carrier recombination. Therefore the photocurrent can be normalised to the number of absorbed photons to calculate the charge generation efficiency, given that the mechanisms which deliver charge carriers are known, i.e. electrode versus bulk generation. We will argue below that for the ITO/SiO$_x$ electrode the photocurrent is due to bulk effects. The normalisation of the photocurrent (fig. 1 (b)) to the number of absorbed photons yields the charge generation efficiency, which is shown in fig. 3. In the device with a bare ITO anode the current is dominated by bulk effects and the normalisation of the corresponding action spectrum (see fig. 1 (a)) results in fig. 4. The quantum yield of intrinsic charge generation is one percent at most for both devices.

Fig. 5 proves that the photocurrent of the bare ITO device is almost temperature independent down to 100 K at an applied electric field of 3x10^5 V/cm. As

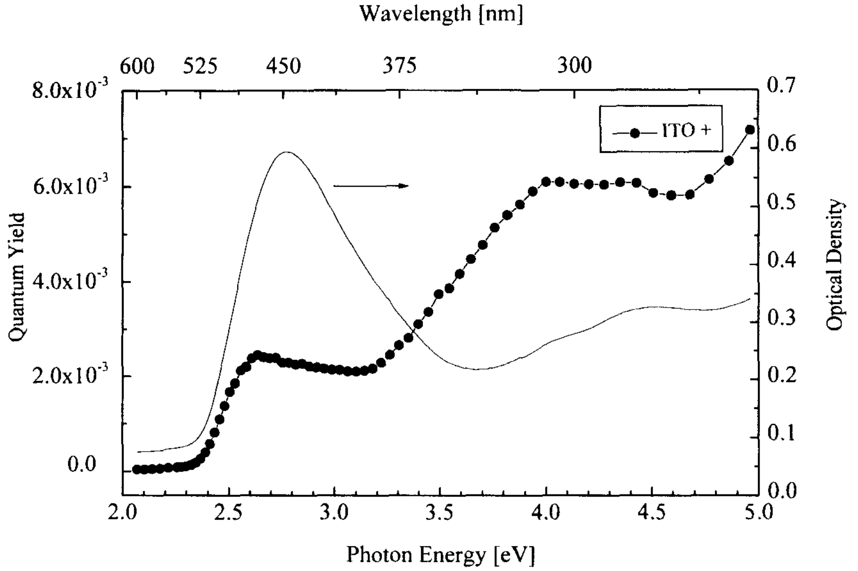

FIGURE 4 The photocurrent measured with a bare ITO anode (fig. 1(a)) normalised to the number of absorbed photons

indicated from fig. 5 the negligible temperature activation is practical independent of the energy of excitation for 2.64 eV and 4.96 eV. Without explicit documentation we note that these phenomena do not change if the ITO is covered with SiO_x.

The electric field dependence of the photocurrent is depicted in fig. 6 on a double logarithmic scale taking into account the built-in potential of the diode resulting from the asymmetry concerning contacting. From the abscissa intercept of the photocurrent-voltage dependence one can conclude that the built-in potential appears with the difference between the Fermi levels of the Al and ITO (0.5 to 0.6 eV). If the ITO is covered with a thin SiO_x layer the built-in potential vanishes. The data points for the bare ITO device at a photon energy of 4.96 eV reflect the dependence of bulk photoionization on electric field, whereas the data for the bare ITO cathode (2.64 eV) correspond to electron injection into the polymer. In both cases the electric field dependence is superlinear.

The photocurrent action spectra at 3.1×10^4 V/cm for a device in surface geometry with interdigitated electrodes is presented in fig. 7. The spectral dependence of the photocurrent is characterised by a pronounced plateau from 2.6 eV to 3.4 eV. It is followed by a steep rise of the current up to 4 eV. Above 4 eV the signal

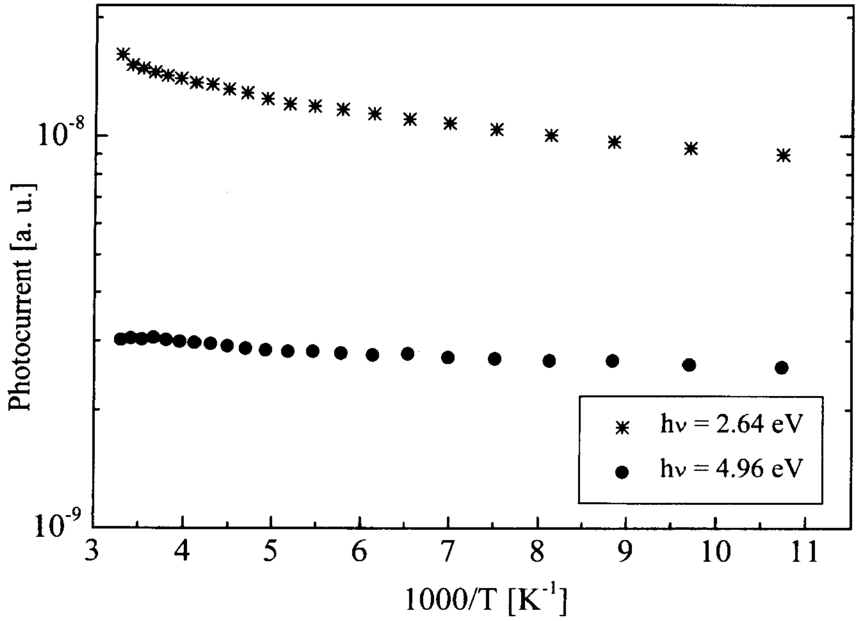

FIGURE 5 Photocurrent of the bare ITO device over 1/T for an applied field of $3x10^5$ V/cm. The excitation energy was 2.64 eV (stars) and 4.96 eV (circles)

detection is limited by the weak intensity of the xenon lamp and the low electric field applied to the interdigitated electrodes.

Finally the efficiency of optical injection of electrons from the ITO under reverse bias is plotted in fig. 8 as a function of photon energy. The yield of this process is obtained by normalising the difference of $j^-(ITO) - j^-(ITO/SiO_x)$ from fig 1(a) and fig 1(b) respectively, according to equation (1) (see discussion section).

4 DISCUSSION

In qualitative terms the experimental results can be summarised as follows: (i) The photocurrent generated upon irradiation through the semitransparent Al electrode is dependent on polarity and electric field but virtually independent on temperature; (ii) for photon energies ≤ 3.2 eV the presence of a SiO_x layer between ITO and CN-PA-PPV has a marked effect on the magnitude of the photocurrent, notably if the ITO is negatively biased; (iii) at photon energies ≤

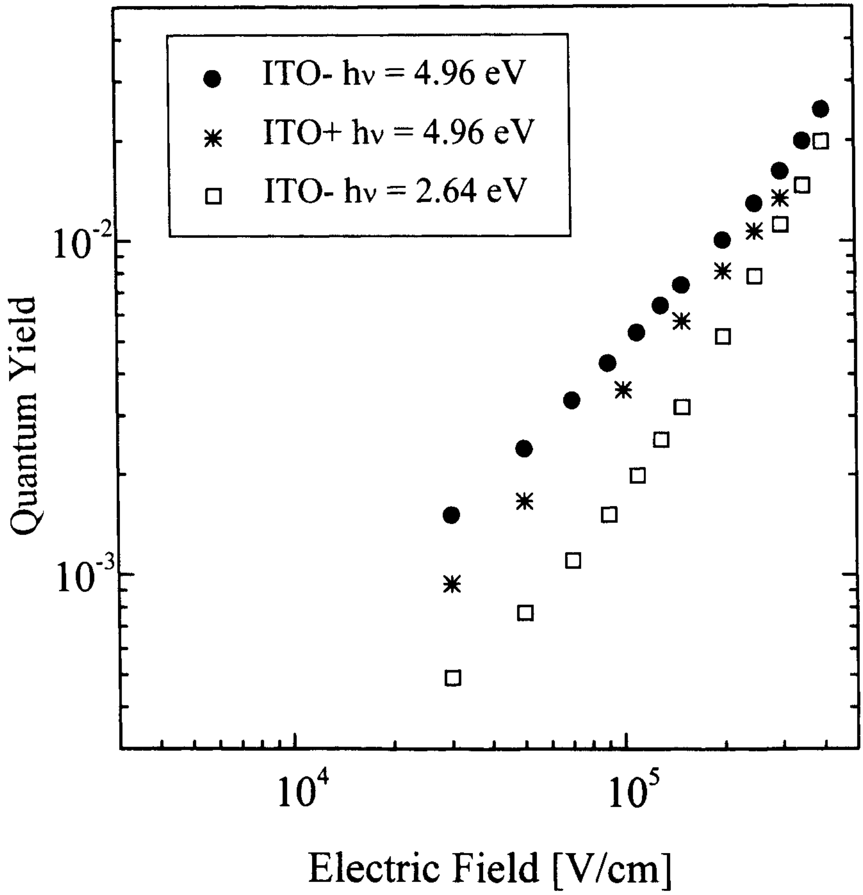

FIGURE 6 Charge generation efficiency vs. electric field. All data were measured with the bare ITO device and corrected for a built-in potential of 0.5 V. The symbols (star, square) refer to ITO being positive or negative (circle)

3.2 eV and positive bias of the ITO/SiO$_x$ electrode the photocurrent is constant but increases for hυ > 3.2 eV approaching a plateau for 3.2 eV < hυ < 4.3 eV followed by a further increase; (iv) for photon energies < 4 eV the action spectrum of the photocurrent measured in a surface cell is coincident with that in a sandwich cell with ITO/SiO$_x$ anode.

From previous experiments on cw-photoconduction on sandwich cells with poly(phenylenevinylene)-ether (PPV-ether) [5] and a ladder-type poly(p-phenylene) (MeLPPP) [11] as a dielectric material contacted with either a bare or

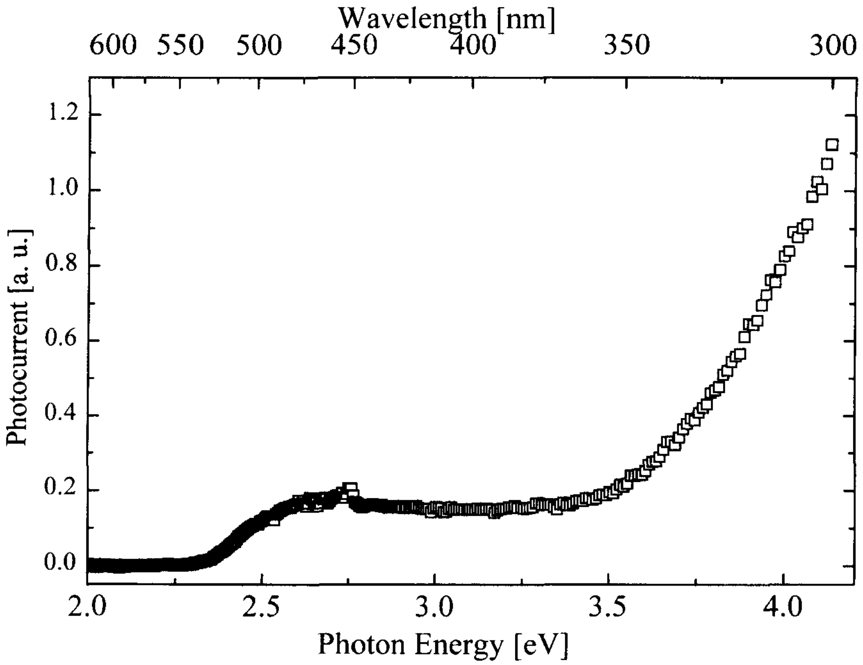

FIGURE 7 The photocurrent action spectrum at 3.1×10^4 V/cm for a device in surface geometry with interdigitated electrodes (gap 160 μm)

SiO_x covered ITO as one of the electrodes it is known that exciton induced hole injection from an ITO anode is the predominant carrier delivering process at photon energies within the vibronic $S_1 \leftarrow S_0$ absorption band. The presence of SiO_x suppresses hole injection, its signature being a photocurrent which is symbatic with absorption if the excitation is done from the ITO side. Injection from the Al electrode is either absent or is negligible relative to bulk generation because optical excitations generated next to a metallic electrode are efficiently quenched due to energy transfer to metal electrons [18]. Based upon these observations it is argued that the photocurrent measured in a sandwich cell with CN-PA-PPV carrying an ITO/SiO_xanode is entirely bulk controlled, if excitation is done through the Al electrode. This is consistent with experiments with a surface cell in which photoinjection at the electrode is excluded. Both action spectra are identical (fig. 1b and 7).

It is less clear what the underlying mechanisms for bulk photogeneration are. The fact that for hv < 3.2 eV the yield is independent of photon energy proves that excess photon energy above the energy of a singlet excitation, i.e. ~ 2.5 eV,

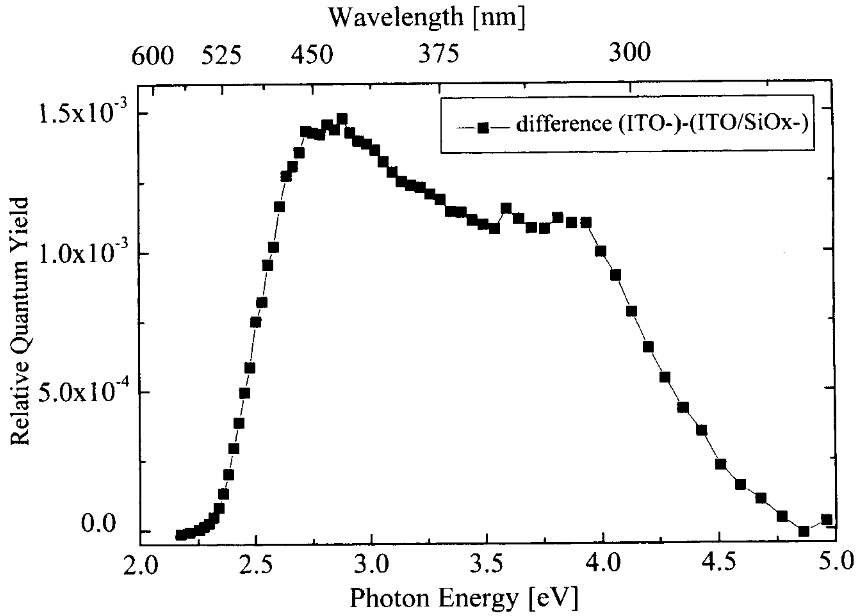

FIGURE 8 The efficiency of electron injection from the ITO cathode, obtained by normalising the difference of j^-(ITO) – j^-(ITO/SiO$_x$) from fig 1(a) and fig 1(b)respectively, according to equation (1)

has no effect, implying that photogeneration proceeds from the vibrationally relaxed singlet exciton. It is open to conjecture, though, if dissociation involves the formation of a precursors geminate electron-hole pair at an adjacent polymer chain or impurity sensitised pair formation. In any event, the yield is on the order of 10^{-3} and increases at higher electric fields while the temperature dependence is virtually negligible. This appears to be a common phenomenon in conjugated polymers and it is incompatible with the conventional Onsager-type photogeneration mechanism which predicts

$$\lim_{T\to\infty}\varphi(E,T)=\lim_{E\to\infty}\varphi(E,T)=\varphi_0$$

where φ_0 is the yield of the initial geminate pair production.

Several models or conjectures have been advanced in order to explain the increase of the bulk photoionization above the singlet exciton energy, which also appears to be a common feature of conjugated polymers, differences being related to the onset at which this process commences. Two of them are based upon the idea that the excess photon energy is used to promote inter-chain photoionization either ballistically [19] or via the heat bath that is temporally generated upon relaxation from an initially hot Franck-Condon state to an equilibrated singlet exciton [20]. In the latter model it is assumed that the relaxed exciton dissociates in terms of a Boltzmann-activated process in which the time dependent effective temperature of the polymer chain is introduced instead of the ambient temperature. It explains the lack of temperature dependence of the photocurrent and predicts a monotonous increase of the yield with increasing photon energy. An intermediate plateau in the yield spectrum would be difficult to explain in terms of the present version of this model unless one would take into account that spatial extension of the initial Franck-Condon states is invoked at higher photon energies [7]. Irrespective of the detailed mechanism by which an hot exciton can use its extra energy in order to overcome the exciton binding energy to dissociate one can conclude that intrinsic photogeneration above the $S_1 \leftarrow S_0$absorption band is an energy consumptive process but does not produce a geminate pair which subsequently dissociates in terms of a field and temperature assisted diffusive random walk inside the coulomb well. Instead a non-thermal, i.e. hot exciton on-chain dissociation has to be invoked. The effect of the electric field is to lower the maximum of the coulomb potential in a given polymer chain similar to a Poole-Frenkel type process, averaged over all orientations of the polymer segments relative to the field. This process is intrinsic in nature and does neither require traps nor disorder.

The effect of a SiO_x layer between ITO and the polymer film will be discussed next. Fig. 1(a) documents that at constant electric field the photocurrent is by a factor of 5 to 6 larger at negative bias of the ITO if the SiO_x layer is absent. Upon opposite bias that enhancement is only a factor of two. By reversing the argument one might argue that photocurrents are lower upon introducing the SiO_x-layer because charges are either injected from the Al electrode or generated in the bulk accumulate at the interface and cause electric field screening. This conjecture can be discarded by the strictly linear intensity dependence of the photocurrent. At higher intensity and, concomitantly, higher current field screening should be more efficient and give rise to a sublinear intensity dependence, at variance with experimental observations (see fig. 2). Another argument against this hypothesis is that the current asymmetry vanishes at photon energies where bulk processes dominate. Therefore one has to conclude that the increase of the photocurrent in a sandwich diode with bare ITO electrode is due to optical injection from the ITO. If so, the action spectrum of the injection process should be determined by the superposition of two phenomena. The number of excitations liable to dissociation at the ITO back electrode should be proportional to the number of excitations produced in a thin slab next to the ITO of thickness of the diffusion length l_d of the excitations. Hence, the injection current should be proportional to the optical density but taking into account the filter effect of the film. Then the hole or electron injection current should follow

$$j^{\pm} = eI_0\varphi^{\pm}\alpha l_d \exp(-\alpha L) \qquad (1)$$

where α is the absorption coefficient, L is the film thickness (implying $L \geq \alpha^{-1}$) and $\varphi^{\pm}$ is the probability that an exciton arriving at the electrode delivers a hole/electron and traverses the sample to the opposite electrode. So far the value of l_d is not known. One can only speculate that it is less than that in the ladder-type poly-para-phenylene (l_d=14 ± 2nm [21]) because CN-PA-PPV is more disordered than MeLPPP as evidenced by the larger inhomogeneous broadening of the absorption. A critical test for this mechanism is that $\varphi^{\pm}$ should be independent of photon energy. Fig. 8 confirms this notion exemplary for j^-. Considering that one has to subtract the photocurrent measured with different samples, i.e. j^-(ITO) – j^-(ITO/SiO$_x$), the agreement is surprisingly good, at least for photon energies hυ ≤ 4 eV. The drop of $\varphi^{\pm}$ for hυ >4 eV might be an indication for the opening of a non-radiative channel for the deactivation of the singlet exciton. However, in the view of the drastic decrease of the light intensity above 4 eV and the concomitant decrease of the absolute photocurrent we are reluctant to draw any further conclusion.

Surprisingly it turns out that electron injection from the ITO into CN-PA-PPV is by a factor of about 5 more efficient than hole injection. Usually it is the opposite. For instance, in PPV-amine, PPV-ether or MeLPPP there was only hole injection from the ITO, consistent with older work on molecular crystals [22]. The distinguishing property appears to be the energetic location of the highest occupied molecular orbital (HOMO) and the lowest unoccupied molecular orbital (LUMO), determined via cyclic voltammetry [16]. Cyano substitution at vinylene groups in PPV increases the oxidation potential by 0.4 to 0.5 eV relative to PPV-amine [23]. Since the energy of the $S_1 \leftarrow S_0$ 0–0 transitions are comparable and tacitly assuming that the exciton binding energies are the same, one can assume that the LUMO level is lower by the same amount. This implies that oxygen or oxidation products which otherwise capture electrons can no longer suppress electron motion. Therefore we conjecture that there is a correlation between the mobility of either holes or electrons and the efficiency of photoinjection not because of differences between the electron coupling at the interface but rather of efficient trapping next to the interface. Though plausible, this conjecture has to be supported by a more systematic study between charge carrier mobility and photoinjection.

In the present context it is appropriate to comment on the notion that SiO$_x$suppresses charge injection. From the present experiments there is good reason to conclude that the photocurrent measured upon shining light through an

$ITO/SiO_x^+/CN-PA-PPV/Al^-$ diode is entirely due to bulk photoionization. Therefore any excess photocurrent observed at reversed polarity has to originate from residual electron injection near the $ITO/SiO_x/CN-PA-PPV$ interface. This is in accord with the fact that the spectral dependence of the current observed with an ITO anode and an ITO/SiO_x cathode are virtually identical, i. e. both must be due to the dissociative exciton diffusion. Obviously, the SiO_x provides some localised states able to capture holes from neutral excited states which subsequently can deliver electrons.

5 CONCLUSIONS

The present results confirm that photogeneration in conjugated polymers is a superposition of three processes, i.e. (i) exciton induced charge injection from an ITO electrode, (ii) bulk photogeneration involving either intrinsic or extrinsic localised states, and (iii) intrinsic intra-chain photogeneration requiring excess photon energy relative to the energy of the S_1 exciton. What is different are the quantum efficiencies of those processes in different polymers. In PPV-amine photoinjection from the ITO is masked by bulk effects completely. It turns out that in ladder-type methyl-substituted poly-phenylene excitonic hole injection from an ITO is by an order of magnitude more efficient than in CN-PA-PPV. The likely reason relates to the high degree of structural order in MeLPPP. It implies that the diffusion length of singlet excitons is larger than in the PPV-type systems and a photogenerated geminate pair forming a hole on a chain and its sibling electron in the ITO is more loosely bound [21]. Evidence for the latter notion comes from the electric field dependence of the injection currents in CN-PA-PPV and MeLPPP. In the case of MeLPPP, $j_{ph}(E)$ saturates at moderate electric fields already, while in CN-PA-PPV the current increases superlinearly. Another qualitative difference between CN-PA-PPV and both MeLPPP and PPV-amine relates to the polarity of majority carrier injection. Although the energy of a singlet excitation would be sufficient to photoinject either an electron or a hole from the ITO, reductive dissociation turns out to prevail in the acceptor-type material and vice versa, probably because of the elimination of trapping effects.

There is growing evidence that in conjugated polymers photogeneration is temperature independent or, at least, very weakly temperature dependent, while the field dependence is strong. This is in disagreement with Onsager-type photodissociation. It indicates that it is the initial, non-thermal event which produces charge carriers from an neutral singlet excitation which is field assisted rather than the diffusive escape of geminate pairs from its mutual Coulombic potential.

Acknowledgements

This work was supported by the Deutsche Forschungsgemeinschaft (SFB 383) and the Fond der Chemischen Industrie.

References

[1] M. Pope, C. E. Swenberg, *Electronic Processes in Organic Crystals and Polymers*, Oxford University Press, New York, (1999).

[2] M. Gailberger, H, Bässler, *Phys. Rev. B* **44**, 8643 (1991).

[3] C. H. Lee, G. Yu, A. J. Heeger, *Phys. Rev.* B **47**, 15 543 (1993).

[4] M. Chandross, S. Mazumdar, S. Jeglinski, X. Wei, Z. V. Vardeny, E. W. Kwock, T. M. Miller, *Phys. Rev.* B **50**, 16 702 (1994).

[5] S. Barth, H. Bässler, H. Rost, H. H. Hörhold, *Phys. Rev.* B **56**, 3844 (1997).

[6] S. Barth, H. Bässler, *Phys. Rev. Lett.* **79**, 4445 (1997).

[7] A. Köhler, D. A. dos Santos, D. Beljonne, Z. Shuai, J.-L. Brédas, A. B. Holmes, A. Kraus, K. Müllen, R. H. Friend, *Nature* (London) **392**, 903 (1998).

[8] S. Barth, H. Bässler, S. Pfeiffer, H. H. Hörhold, *Macromol. Chem. Phys.* **199**, 717 (1998).

[9] M. G. Harrison, J. Grüner, G. C. W. Spencer, *Phys. Rev.* B **55**, 7831 (1997).

[10] T. K. Däubler, H. Rost, H. H. Hörhold, D. Neher, *Phys. Rev.* B **59**, 1964 (1999).

[11] S. Barth, H. Bässler, U. Scherf, K. Müllen, *Chem. Phys. Lett.* **288**, 147 (1998).

[12] B. Mulder, *Philips Res. Rep.* **4**, 1 (1968).

[13] K. Kato, C.L. Braun, *J. Chem. Phys.* **72**, 172 (1980).

[14] C. H. Lee, G. Yu, D. Moses, K. Pakbaz, C. Zhang, N. S. Sariciftci, A. J. Heeger, F. Wudl, *Phys. Rev.* B **48**, 15 425 (1993).

[15] H.-H. Hörhold, H. Liebegott, H. Tillmann, A. Hartmann, J. Nowotny, D. Raabe, R. Stockmann, *SPIE Conference* **3476**-10 (1998). H. Tillmann, H.-H. Hörhold, *37. IUPAC-Congress* (1999), Berlin, Book of Abstracts 694.

[16] Elemental analysis $(C_{46}H_{51}N_3O_2)_n$ $(677.89)_n$ Calc.: C 81.49 H 7.58 N 6.20 Found: C 81.07 H 8.15 N 6.13 Molecular weight: $M_n = 5.800$ (GPC), $M_w = 15.600$ (GPC), $M_n = 8.500$ (VPO). FT-IR (KBr): $\upsilon/\mathrm{cm}^{-1}$3036 (Ph), 2925 and 2855 (CH_3), 2211 (CN), 1585 and 1504 (Ph breathing), 1213 and 1026 (Ph-O-C). ^{13}C NMR (100 MHz, $CDCl_3$) δ/ppm 150.5; 148.7; 146.0; 145.7; 130.7; 129.8; 128.4; 126.4; 125.6; 125.4; 122.9; 118.5; 114.3; 105.6; 69.7; 31.7; 29.3; 29.26; 29.23; 26.2; 22.6; 14.1. ^1H NMR (400 MHz, $CDCl_3$) δ/ppm 7.81 (d; H^4), 7.64 (s; H^2), 7.37–6.90 (m; H^{11}), 4.05 (t; H^4), 1.85–1.23 (m; H^{24}), 0.84 (t; H^6). $E_{ox} = 1.12$ V (Ag/AgCl).

[17] H. E. Wolf, *Silicon Semiconductors Data*, Pergamon Press, London, 1969.

[18] G. Vaubel, H. Bässler, D. Möbius, *Chem. Phys. Lett.* **10**, 334 (1971).

[19] V.I. Arkhipov, E. V. Emelianova, H. Bässler, *Chem. Phys. Lett.* **296**, 452 (1998).

[20] V.I. Arkhipov, E. V. Emelianova, H. Bässler, *Phys. Rev. Lett.* **82**, 1321 (1999).

[21] A. Haugeneder, M. Neges, C. Kallinger, W. Spirkl, U. Lemmer, J. Feldmann, U. Scherf, E. Harth, A. Gügel, K. Müllen, *Phys. Rev.* B **59**, 15 346 (1999).

[22] H. Bässler, H. Killesreiter, G. Vaubel, *Discuss. Faraday Soc.* **51**, 48 (1971).

[23] S. Pfeiffer, H. Rost, H. H. Hörhold, *Macromol. Chem. Phys.* **200**, 2471 (1999).